

Electronic Supplementary Information

Coexistence of fluorescent *Escherichia coli* strains in millifluidic droplets reactors

Xinne Zhao,^{ab} Rico Illing,^{ac} Philip Ruelens,^d Michael Bachmann,^b Gianarelio Cuniberti,^{*a}

J. Arjan G. M. de Visser,^d and Larysa Baraban^{*ab}

X. Zhao, Dr. R. Illing, Prof. G. Cuniberti, Dr. L. Baraban
Institute for Materials Science and Max Bergmann Center of Biomaterials,
Technische Universität Dresden, 01062 Dresden, Germany.
E-mail: gianarelio.cuniberti@tu-dresden.de

X. Zhao, Dr. L. Baraban
Helmholtz-Zentrum Dresden Rossendorf, Institute of Radiopharmaceutical Cancer
Research, Bautzner Landstraße 400, 01328 Dresden, Germany.
E-mail: l.baraban@hzdr.de

Dr. R. Illing
Helmholtz-Zentrum Dresden Rossendorf, Institute of Ion Beam Physics and Materials
Research, Bautzner Landstraße 400, 01328 Dresden, Germany.

Prof. A. de Visserd, Dr. P. Ruelensd
Department of Genetics, Wageningen University, Arboretumlaan 4, 6703 BD
Wageningen, The Netherlands

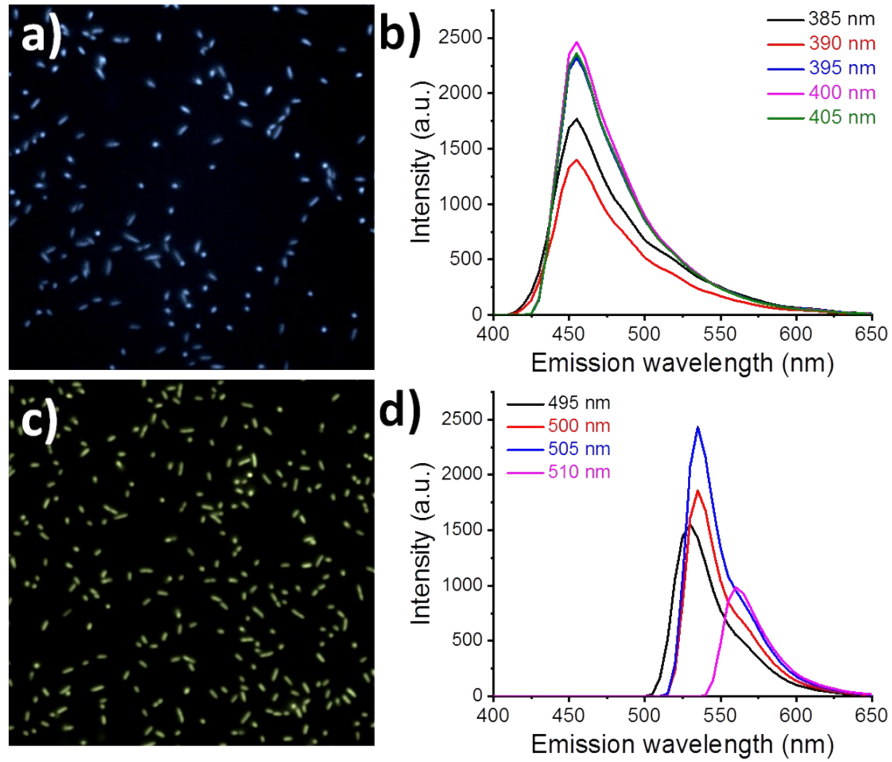


Fig. S1 Fluorescence detection of *E. coli* BFP and *E. coli* YFP: a) *E. coli* BFP observed under a fluorescence microscope and excited by UV light with a magnification of 100 \times ; b) the fluorescence emission spectrum of *E. coli* BFP excited by a different wavelength of the light source. c) *E. coli* YFP observed under a fluorescence microscope and excited by blue light with a magnification of 100 \times ; d) the fluorescence emission spectrum of *E. coli* YFP excited by a different wavelength of the light source.

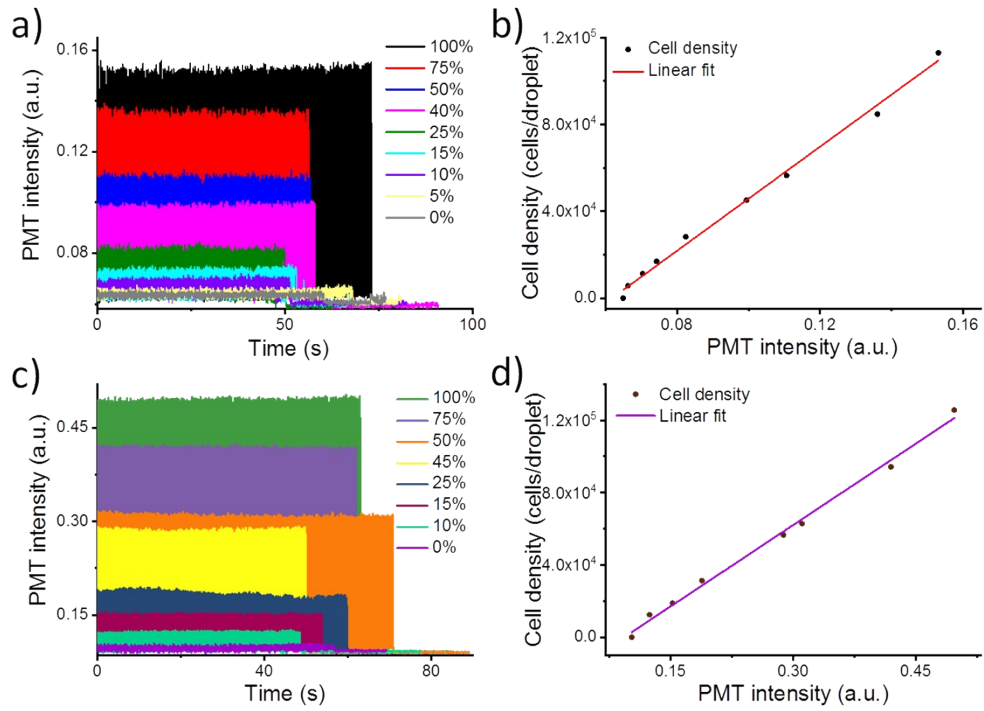


Fig. S2 Calibration curves for Multiple Fluorescence Droplet Analyzer (FDA) of *E. coli* BFP and *E. coli* YFP. The signal of a) several droplet sequences with a known concentration and b) the final calibration curve for the *E. coli* BFP and the same signal for *E. coli* YFP c) and d) in M9 media.

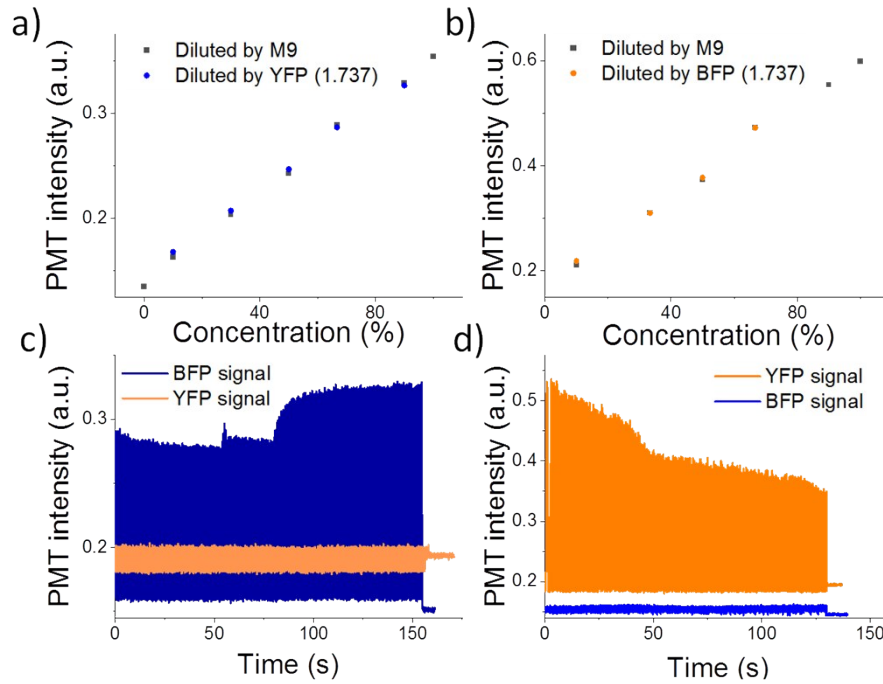


Fig. S3 Comparison of single strain and mixed strains signal for Multiple Fluorescence Droplet Analyzer (FDA) of *E.coli BFP* and *E.coli YFP*. a) BFP signal (black dots) with different concentrations diluted by M9 as the ratio of 9:1, 2:1, 1:1, 1:2, and 1: 9 (the original BFP cell density OD 600 = 1.737 A), and BFP signal (orange dots) with different concentrations mixed with YFP as the ratio 9:1, 2:1, 1:1, 1:2, and 1: 9 (original BFP and YFP cell density are the same, OD600 = 1.737 A). b) YFP signal (black dots) with different concentrations diluted by M9 as the ratio of 9:1, 2:1, 1:1, 1:2, and 1: 9 (the original YFP cell density OD 600 = 1.737 A), and YFP signal (blue dots) with different concentrations mixed with BFP as the ratio 9:1, 2:1, 1:1, 1:2, and 1: 9 (original BFP and YFP cell density are the same, OD600 = 1.737 A). c) The real-time signal of the droplet sequence contains *E.coli BFP* and *E.coli YFP* with the cell density ratio tuned from 100:1 to 900:1, and caught by two detection modes (the blue line represents BFP signal, the orange line represents YFP signal). d) The real-time signal of the droplet sequence contains *E.coli BFP* and *E.coli YFP*, with the cell density ratio tuned from 1:900 to 1:100 and caught by two detection modes (the blue line represents BFP signal, the orange line represents YFP signal).

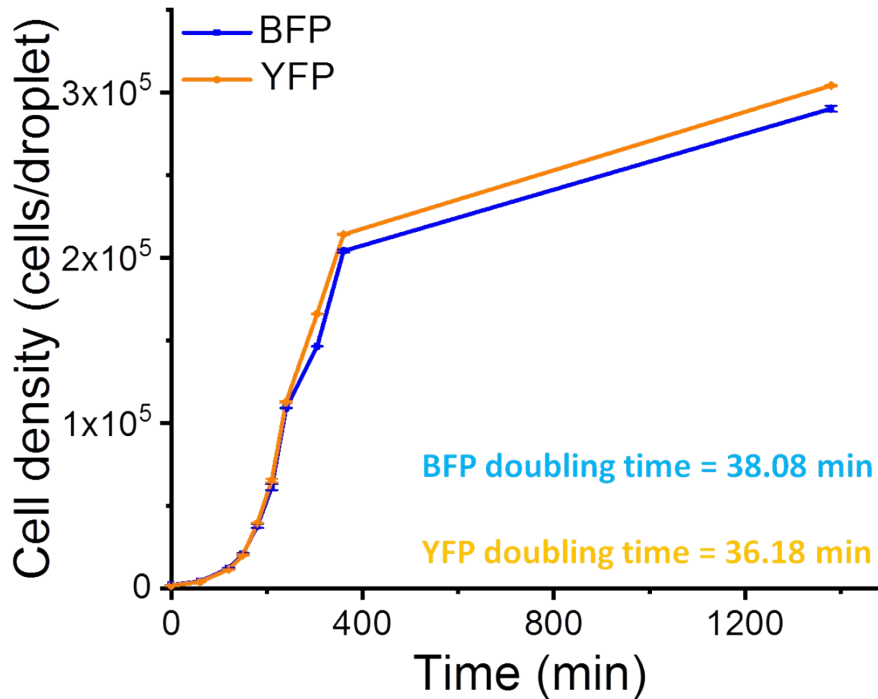


Fig. S4 Growth curves of *E. coli BFP* (blue line) and *E. coli YFP* (yellow line) obtained by batch culture method and measured with OD 600.

In Fig. S4, the optical density of both bacterial strains was measured every 60 min; from the 2nd h to 4th h, the measurement was taken every 30 min. The final cell density of *E. coli YFP* reaches a high point around 1.5×10^9 cells/mL, which is slightly higher than *E. coli BFP* 1.4×10^9 cells/mL. However, the doubling time of *E. coli BFP* is calculated to be 38.08 min, which is slower than *E. coli YFP* 36.18 min. Overall, the batch culture method results suggested the growth rate of *E. coli YFP* is faster than *E. coli BFP*. Besides, the final population size of *E. coli YFP* is also larger than *E. coli BFP* in the same culturing environment.

Notable among the *E. coli YFP* monoculture growth curves is the decrease of fluorescence signal after 1000 min, which can be attributed to the photobleaching, and was not observed in the *E. coli BFP* case or the batch culture method.¹ Due to the limit of nutrients in medium and a long time shined under a light source, the YFP became unstable or even damaged. Especially when the cells are no longer dividing and replacing their fluorophores, the cells get aged. Their YFP activity decreases over time, leading to the drop of fluorescence intensity; thus, irreversible photobleaching occurred.² The typical growth curve of *E. coli* is S-shaped (cell number vs. incubation time). Either through optical density detection³ or other detection methods such as electrical sensor⁴ and our fluorescent millifluidic sensor, the cell number detected is the total number accumulation, but not the net live cell number. During the stationary phase, the number of new cells equals the number of dead cells so that there is no net increase in viable cells. The dead cells and new dividing cells accumulate together, making the growth curve a slight increase in the stationary phase. From the monoculture growth curves obtained by flow cytometry counting, optical density absorption analysis, and plate reader counting in Fig. S5 a-d, all the growth curves of

E. coli BFP slightly go up in the stationary phase. In another word, all the methods mentioned here measured the accumulation of the total number of cells (both dead and alive), but not the net increase in viable cells. Except for the *E. coli YFP* growth curves measured by plate reader decline as the same as in millifluidic droplet reactor, the *E. coli YFP* growth curves measured by other methods in the stationary phase have the same increase trend as *E. coli BFP*. In Fig. S5 e and f, compared to the Cmax of *E. coli BFP* (blue dotted line), the *E. coli BFP* incubated in PBS (light blue curves) remains unchanged in the stationary phase while going up in M9 media (purple curves). Besides, compared to the Cmax of *E. coli YFP* (orange dash line), the *E. coli YFP* incubated in PBS (orange curves) slightly decreased but not as obvious as *E. coli YFP* in M9 decreased (yellow curves), might due to the photobleaching happens stronger to dead cells than to alive cells. The signal difference between *E. coli* incubated in the M9 media and the PBS media is because after washing and incubating bacteria by PBS media, the environmental effects are eliminated; for example, during the stationary phase, nutrients and oxygen levels are becoming depleted, the pH is changing, and toxic wastes are building up. The relationship between the fluorescent signals and the cell number is verified by measuring pH value, cell size, and alive/dead cell after incubating for 0, 9, 24, and 36 h (Fig. S6). The results show that both strains' cell size didn't change during cultivation, while pH value and viable cell rate dropdown.

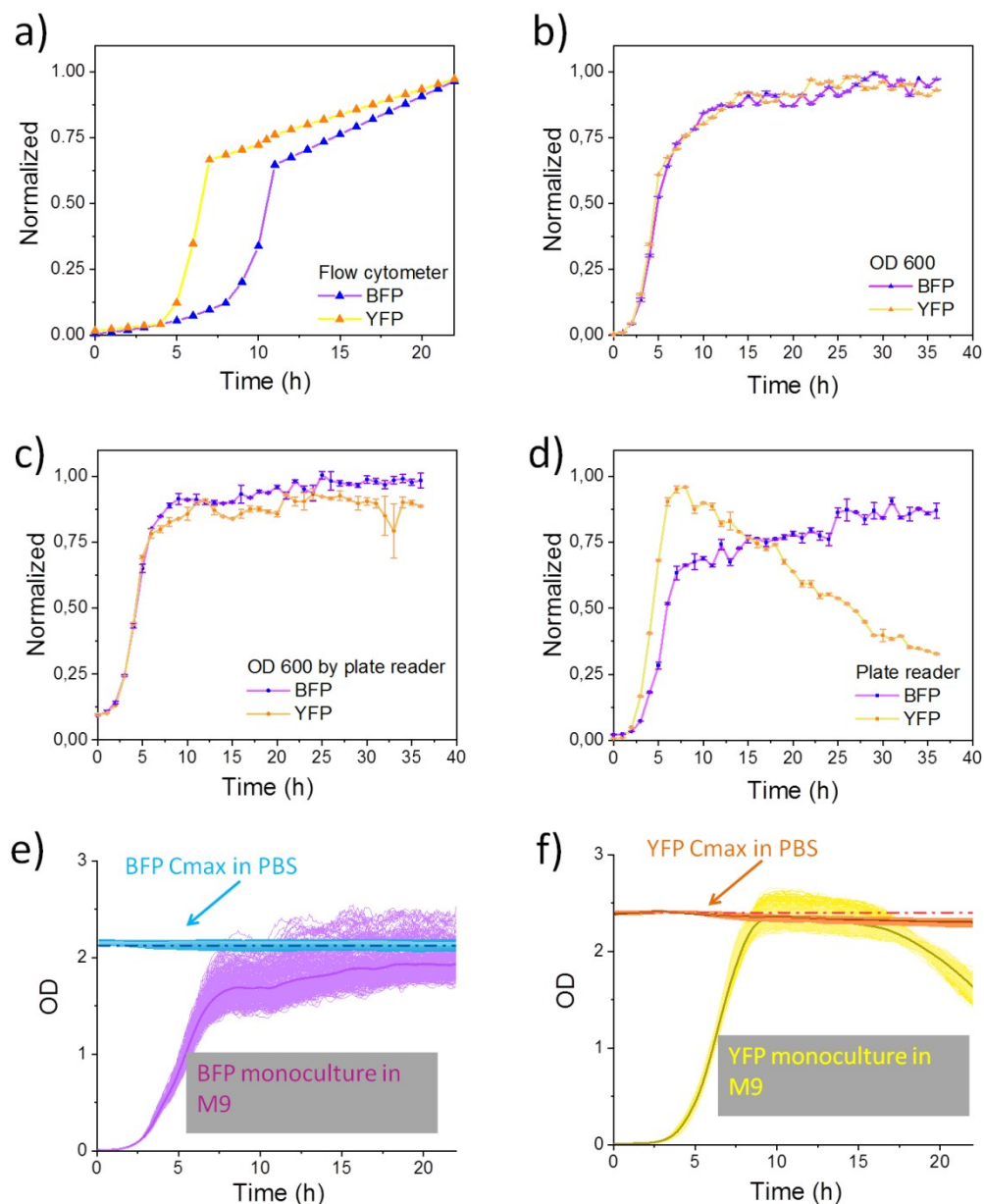


Fig. S5 The growth curves of *E. coli* BFP (blue line) and *E. coli* YFP (yellow line) measured by a) flow cytometer, b) photometer, c) plate reader measured optical density, and d) plate reader measured fluorescent signal. The changes in the fluorescence signals of *E. coli* incubated in different media in millifluidic device: e) the growth curves of *E. coli* BFP incubated in M9 media (purple curves) and PBS media (light blue curves, *E. coli* is first batch cultured to maximum cell concentration C_{max} and then centrifuged and incubated into PBS medium with cell concentration of C_{max}), and the C_{max} of *E. coli* BFP (blue dash line). f) The growth curves of *E. coli* YFP incubated in M9 media (yellow curves) and PBS media (orange curves) and the C_{max} of *E. coli* YFP (orange dash line).

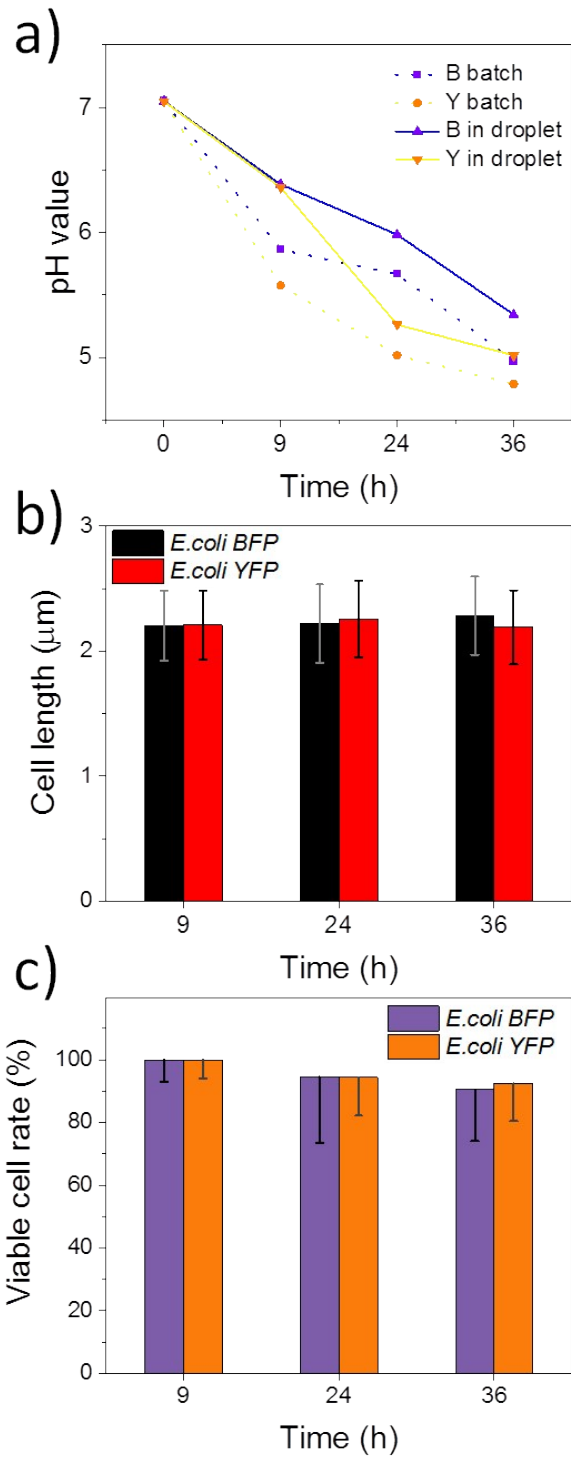


Fig. S6 Comparison of a) pH value in batch culture and in droplets, b) cell size, and c) viable cell rate after incubating bacteria for 0 h, 9 h, 24 h, and 36 h.

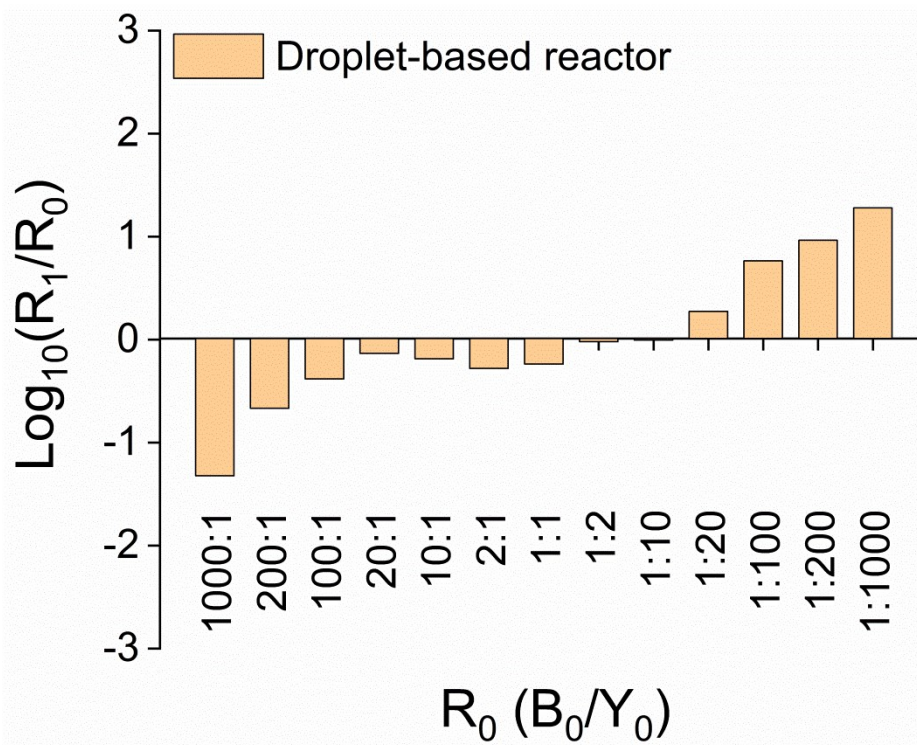


Fig. S7 The relationship between ratio fold change $\log_{10}(R_1/R_0)$ and R_0 . ($R_0 = B_0/Y_0$, the initial biomass ratio between *E.coli BFP* and *E.coli YFP*; $R_1 = B_1/Y_1$, the biomass ratio (at the beginning of stationary phase between *E.coli BFP* and *E.coli YFP*).

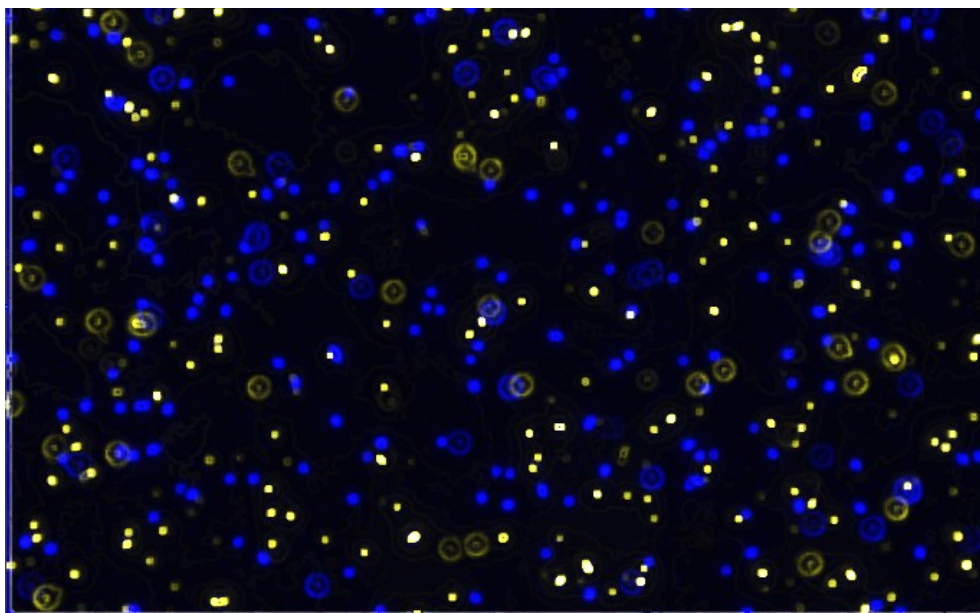
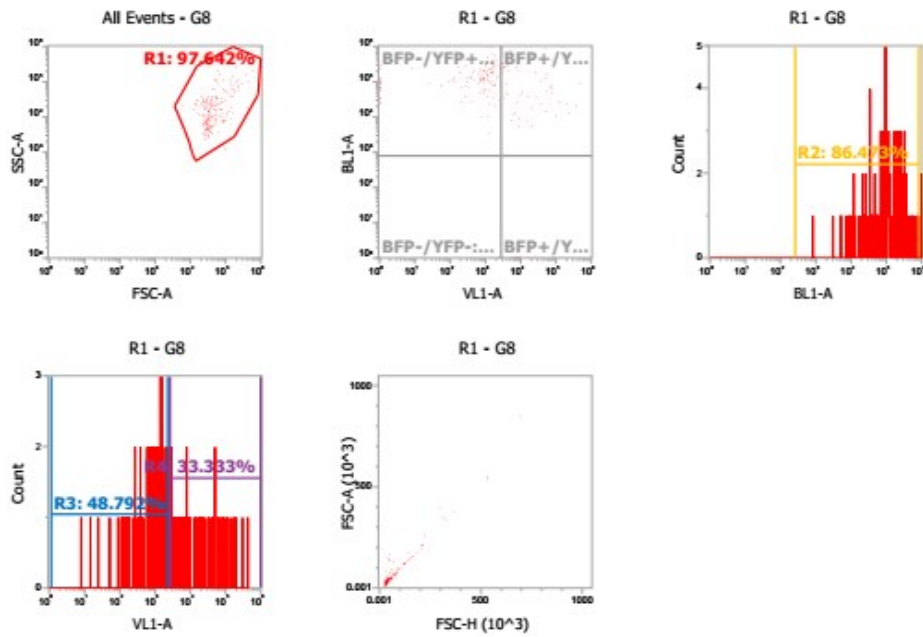


Fig. S8. The merged graph of *E.coli BFP* and *E.coli YFP* observed with a fluorescence microscope excited by UV light and blue light separately with a magnification of 40 \times .



Parameters: **VL1-A vs BL1-A**
 Gate: **All Events**
 Experiment: **Experiment**
 Group: **Group**
 Sample: **G8**
 Time Recorded: **14:09:30**

| Name | Gate | X Parameter | Y Parameter | Count | %Total | %Gated |
|------------|------------|-------------|-------------|-------|---------|---------|
| All Events | All Events | VL1-A | BL1-A | 212 | 100.000 | 100.000 |
| R1 | R1 | VL1-A | BL1-A | 207 | 97.642 | 97.642 |
| BFP-/YFP+ | BFP-/YFP+ | VL1-A | BL1-A | 132 | 62.264 | 63.768 |
| BFP+/YFP+ | BFP+/YFP+ | VL1-A | BL1-A | 51 | 24.057 | 24.638 |
| BFP-/YFP- | BFP-/YFP- | VL1-A | BL1-A | 8 | 3.774 | 3.865 |
| BFP+/YFP- | BFP+/YFP- | VL1-A | BL1-A | 16 | 7.547 | 7.729 |

Fig. S9 Result report screenprint of the flow cytometer software ($R_0 = 10^{-3}$).

Table S1 Cell numbers and R_1 with different R_0 measured by flow cytometer.

| R_0 | B_1 | Y_1 | R_1 |
|-----------|-------|-------|--------|
| 1000:1 | 11 | 325 | 29.545 |
| 1000:5 | 14 | 391 | 27.929 |
| 1000:10 | 13 | 331 | 25.462 |
| 1000:50 | 7 | 70 | 10.000 |
| 1000:100 | 15 | 90 | 6.000 |
| 1000:500 | 31 | 81 | 2.613 |
| 1000:1000 | 137 | 113 | 0.825 |
| 500:1000 | 22 | 22 | 1.000 |
| 100:1000 | 61 | 22 | 0.361 |
| 50:1000 | 199 | 55 | 0.276 |
| 10:1000 | 138 | 14 | 0.101 |
| 5:1000 | 161 | 24 | 0.149 |
| 1:1000 | 132 | 16 | 0.121 |

Table S2 Cell numbers and R_1 with different R_0 measured by a plate reader.

| R_0 | B_1 10^8 cell/mL | Y_1 10^8 cell/mL | R_1 |
|-----------|-------------------------|-------------------------|--------|
| 1000:1 | 5.360 | 0.299 | 17.925 |
| 1000:5 | 5.370 | 0.325 | 16.502 |
| 1000:10 | 5.530 | 0.365 | 15.126 |
| 1000:50 | 5.740 | 0.696 | 8.246 |
| 1000:100 | 5.330 | 0.959 | 5.555 |
| 1000:500 | 4.400 | 3.080 | 1.429 |
| 1000:1000 | 3.870 | 4.550 | 0.851 |
| 500:1000 | 2.250 | 5.110 | 0.441 |
| 100:1000 | 0.800 | 5.350 | 0.150 |
| 50:1000 | 0.484 | 5.600 | 0.086 |
| 10:1000 | 0.297 | 5.900 | 0.050 |
| 5:1000 | 0.277 | 6.190 | 0.045 |
| 1:1000 | 0.312 | 6.390 | 0.049 |

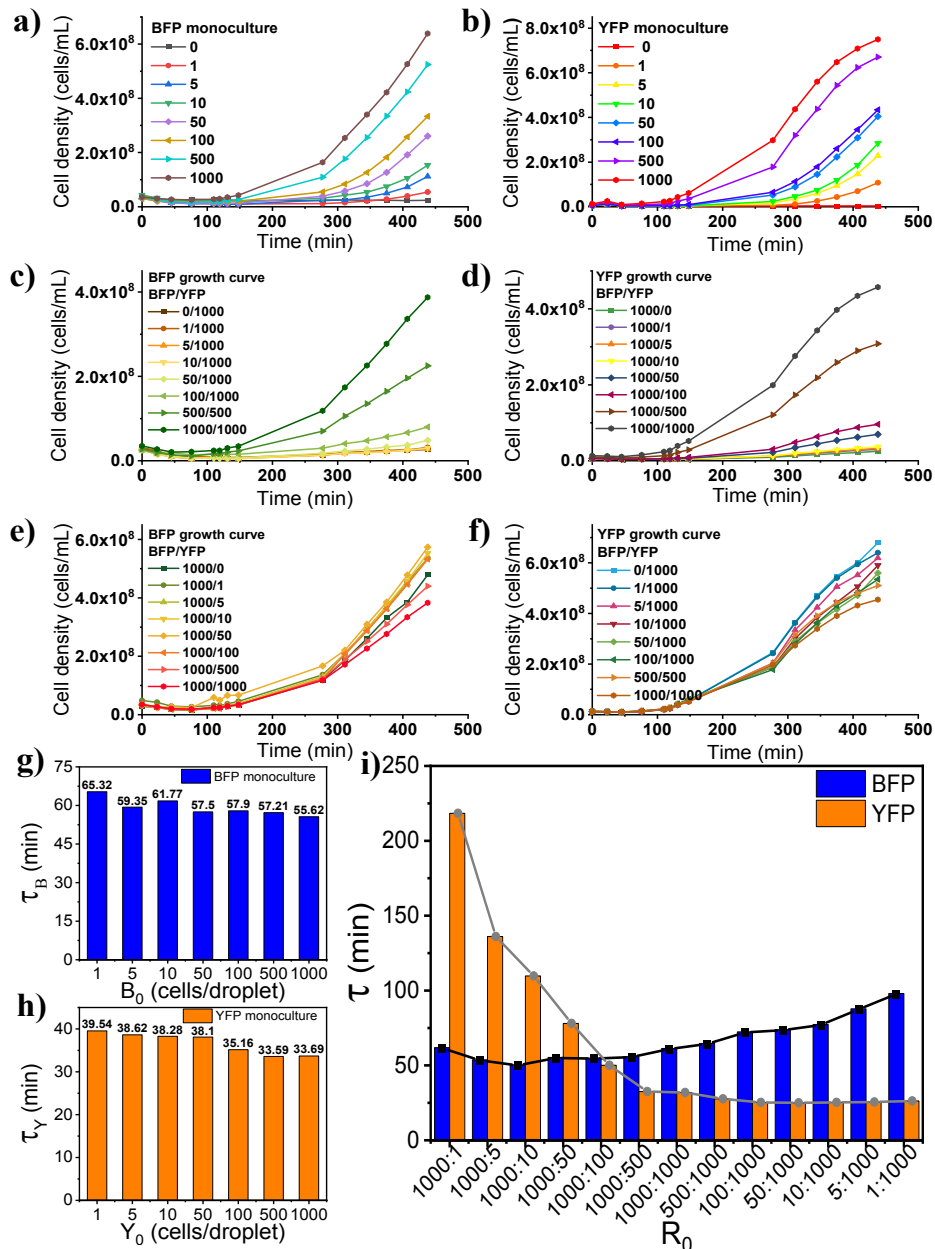


Fig. S10 Comparison of the growth curves and doubling time of two strains bacterial. The growth curves of a) *E.coli* BFP monoculture with initial cell density of 0, 1, 5, 10, 50, 100, 500, and 1000 cells/droplet; b) *E.coli* YFP monoculture with initial cell density of 0, 1, 5, 10, 50, 100, 500, and 1000 cells/droplet; c) *E.coli* BFP with initial cell density of 1, 5, 10, 50, 100, 500, and 1000 cells/droplet co-culture with 1000 cells/droplet of *E.coli* YFP; d) *E.coli* YFP with initial cell density of 1, 5, 10, 50, 100, 500, and 1000 cells/droplet co-culture with 1000 cells/droplet of *E.coli* BFP; e) 1000 cells/droplet initial cell density of *E.coli* BFP co-culture with 1, 5, 10, 50, 100, 500, and 1000 cells/droplet *E.coli* YFP; f) 1000 cells/droplet initial cell density of *E.coli* YFP co-culture with 1, 5, 10, 50, 100, 500, 1000 cells/droplet *E.coli* BFP. The doubling time of g) *E.coli* BFP and h) *E.coli* YFP monoculture with initial cell density of 1, 5, 10, 50, 100, 500, and 1000 cells/droplet. i) Comparison of doubling time between two strains of *E.coli* with different R_0 from 1000:1 to 1:1000.

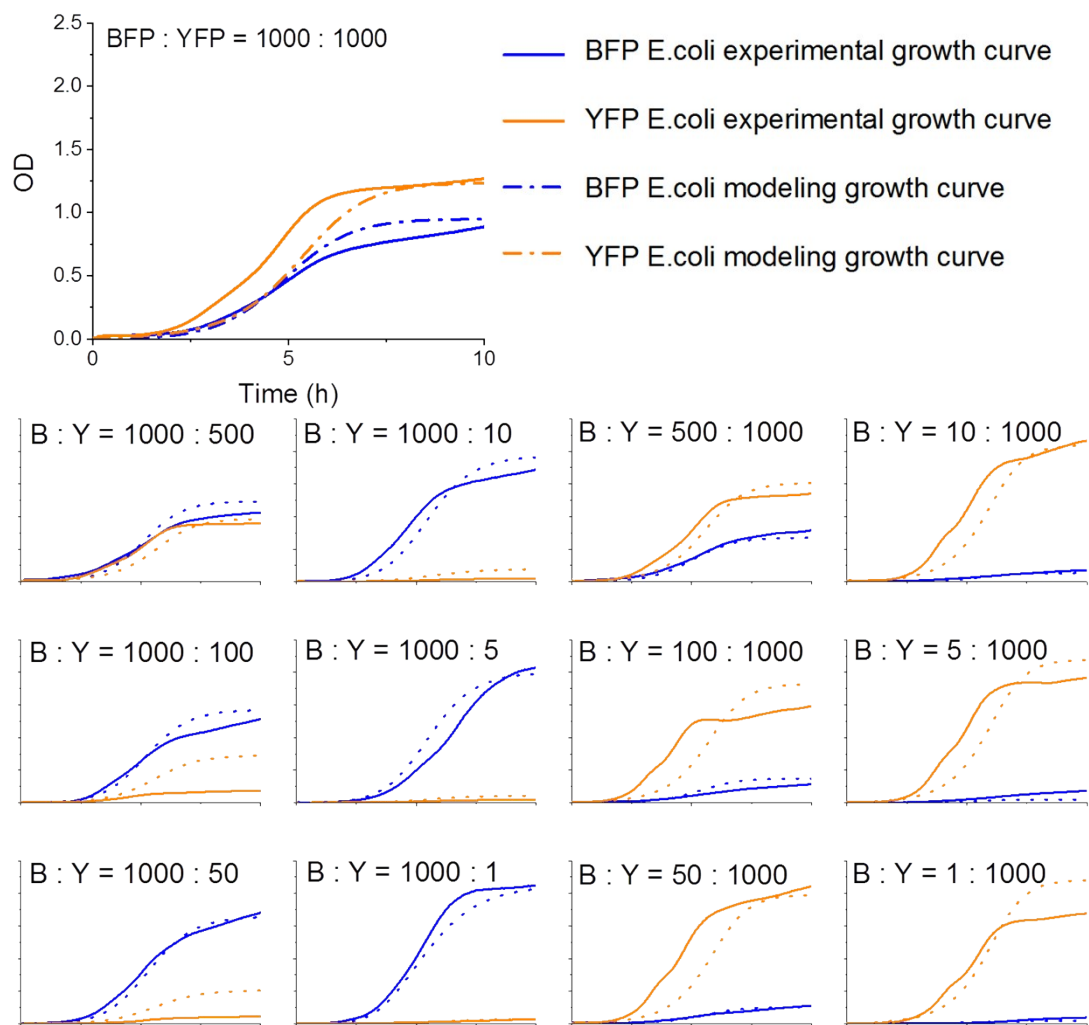


Fig. S11 The comparison of experimental growth curves and modeling growth curves of co-culture *E.coli* BFP and *E.coli* YFP.

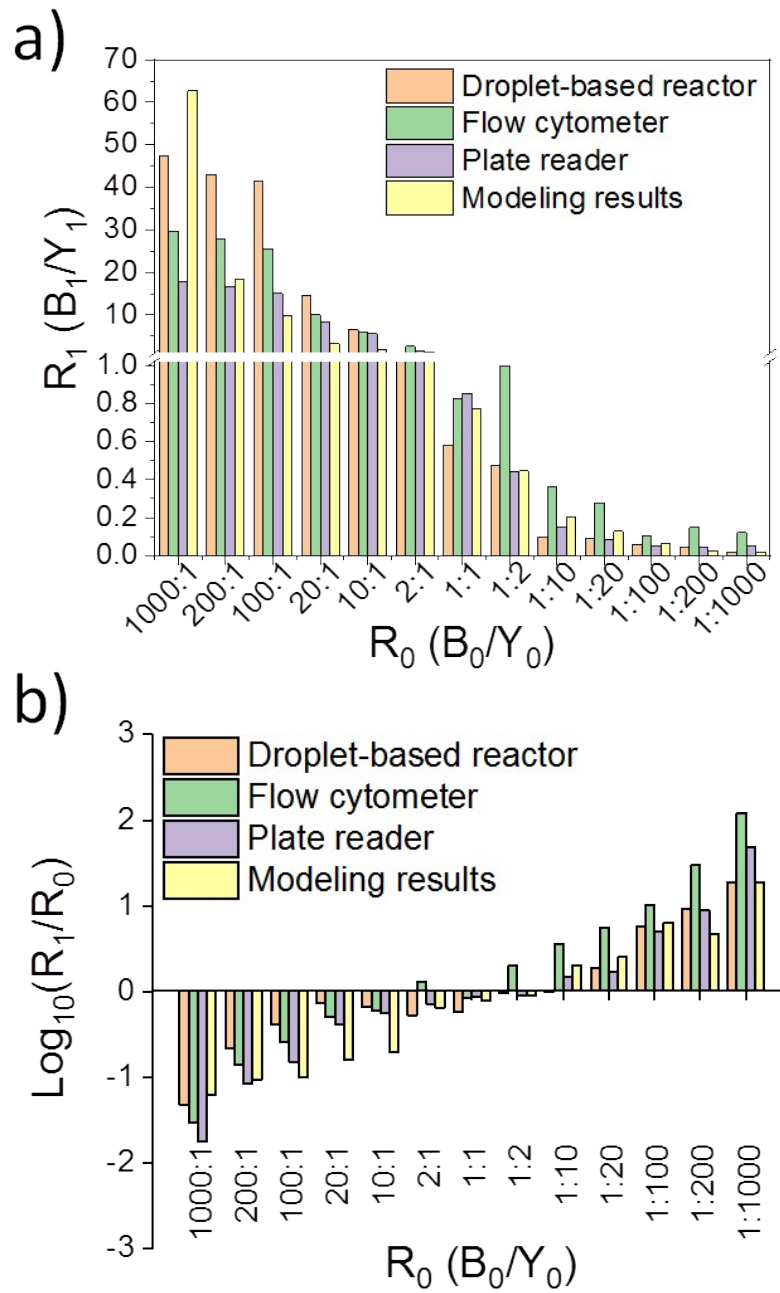


Fig. S12 Comparison of R_1 and R_0 between two strains of *E. coli* measured by different methods. a) The R_1 changes with various R_0 ; b) The relationship between ratio fold change $\text{log}_{10}(R_1/R_0)$ and R_0 .

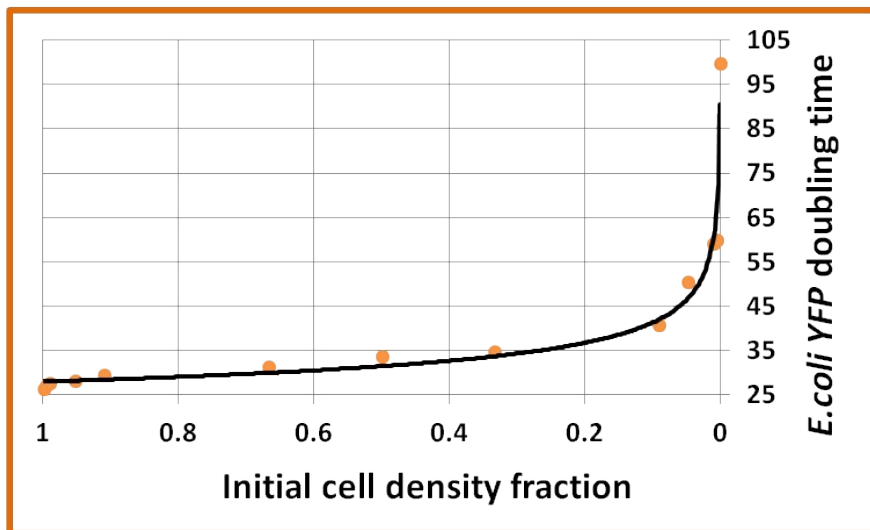
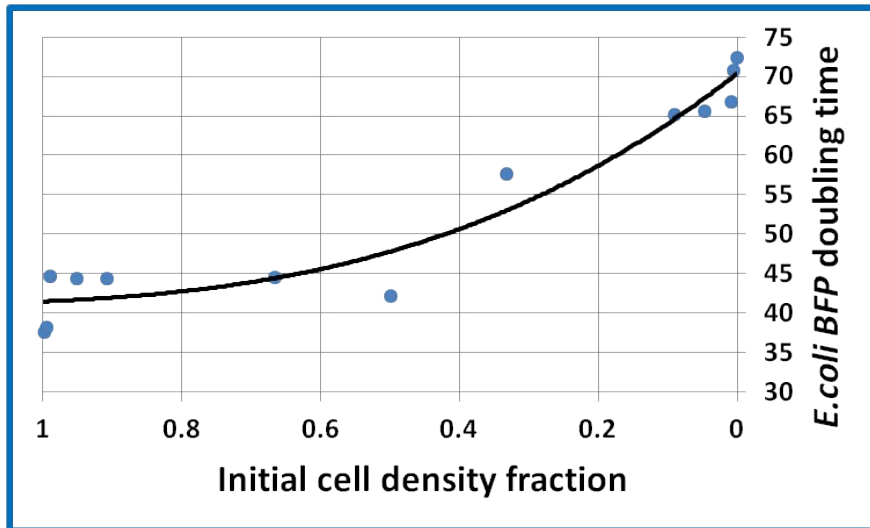


Figure S13. The development of doubling time changing with the decrease of initial cell density fraction: a) *E.coli BFP* and b) *E.coli YFP*.

For *E.coli BFP*, the function is close to polynomial function, and *E.coli YFP* is close to power function (shown in Figure S13).

$$y = -14.447 x^3 + 54.192 x^2 - 68.67 x + 70.365 \quad (E.coli \ BFP, \ R^2 = 0.9423) \quad (1)$$

$$y = 27.949 x^{-0.17} \quad (E.coli \ YFP, \ R^2 = 0.9748) \quad (2)$$

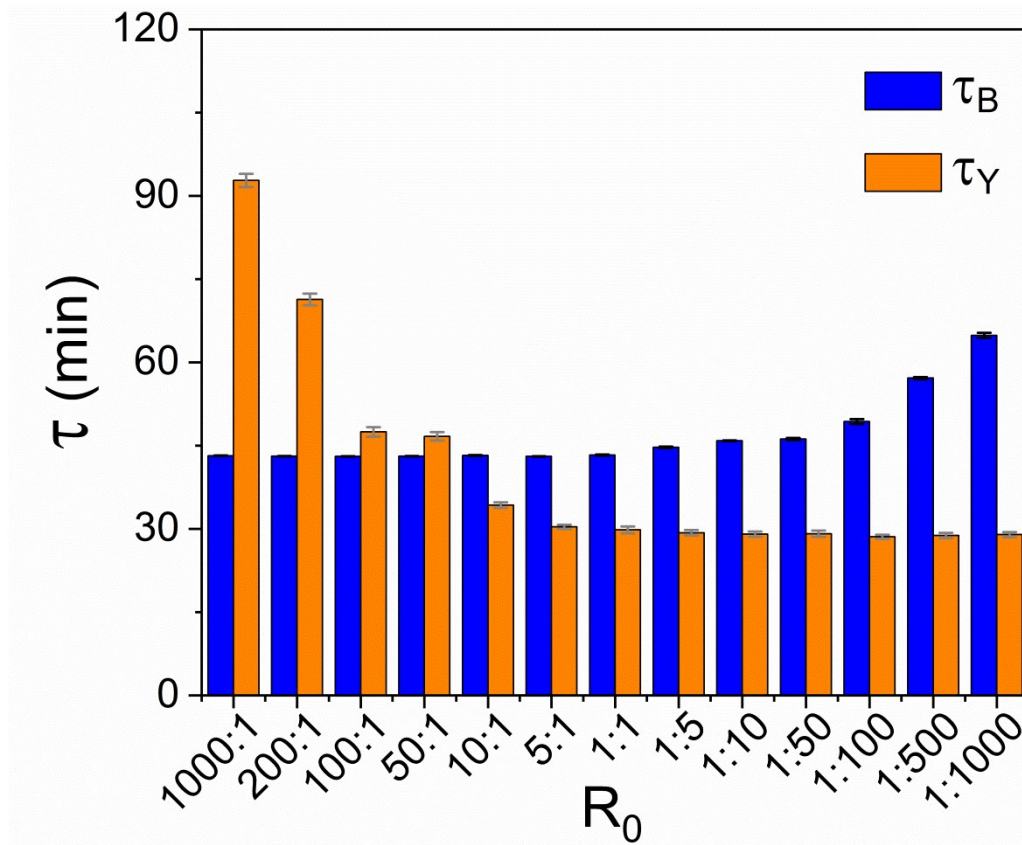


Fig. S14 Comparison of the modeling result of doubling time between two strains of *E.coli* with different R_0 from 10^3 to 10^{-3} .

Table S3 Distribution statistics of dots with different R_0 in four regions (in monoculture and co-culture cases).

| R_0 | Monoculture (%) | | | | | Co-culture (%) | | | | |
|-----------|-----------------|------------------|-----------------|-------------|-------|----------------|------------------|------------------|-------------|-------|
| | Mutualism | Domination_ Y | Dmination_ B | Competition | Total | Mutualism | Domination_ Y | Domination_ B | Competition | Total |
| | 1000:1 | 32.22 | 11.37 | 18.01 | 18.01 | 422 | 0.00 | 0.00 | 70.99 | 29.01 |
| 1000:5 | 30.57 | 14.69 | 19.91 | 34.12 | 422 | 0.23 | 0.00 | 81.25 | 18.52 | 432 |
| 1000:10 | 21.90 | 15.83 | 23.48 | 38.79 | 420 | 0.00 | 0.00 | 0.00 | 100.00 | 379 |
| 1000:50 | 34.86 | 14.66 | 15.63 | 35.01 | 416 | 0.00 | 0.00 | 0.00 | 100.00 | 406 |
| 1000:100 | 39.04 | 10.12 | 10.84 | 40.00 | 415 | 0.00 | 10.17 | 0.00 | 89.83 | 423 |
| 1000:500 | 10.19 | 37.91 | 36.49 | 10.19 | 422 | 0.00 | 2.27 | 0.00 | 97.73 | 396 |
| 1000:1000 | 39.34 | 12.56 | 11.14 | 36.97 | 422 | 0.24 | 4.33 | 12.02 | 83.41 | 416 |
| 500:1000 | 27.27 | 25.17 | 27.04 | 20.51 | 429 | 0.00 | 96.46 | 0.00 | 2.78 | 396 |
| 100:1000 | 31.93 | 20.51 | 18.18 | 29.37 | 429 | 0.00 | 100.00 | 0.00 | 0.00 | 432 |
| 50:1000 | 27.51 | 25.17 | 12.12 | 35.20 | 429 | 0.00 | 100.00 | 0.00 | 0.00 | 425 |
| 10:1000 | 27.75 | 28.25 | 25.50 | 23.75 | 400 | 0.00 | 100.00 | 0.00 | 0.00 | 397 |
| 5:1000 | 13.05 | 39.16 | 36.60 | 11.19 | 429 | 0.00 | 100.00 | 0.00 | 0.00 | 422 |
| 1:1000 | 25.76 | 26.23 | 21.55 | 25.76 | 427 | 0.00 | 100.00 | 0.00 | 0.00 | 412 |

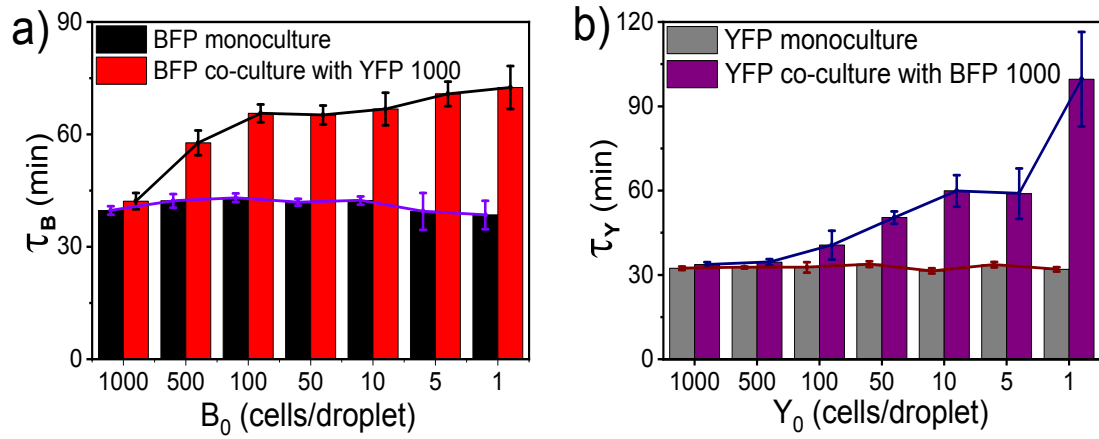


Fig. S15 a) Comparison of doubling time of *E. coli* BFP with different initial cell density in a monoculture environment and co-culture with initial cell density 1000 cells/droplet *E. coli* YFP. b) Comparison of doubling time of *E. coli* YFP with different initial cell density in a monoculture environment and co-culture with initial cell density 1000 cells/droplet *E. coli* BFP. Error bars show the standard error of the mean.

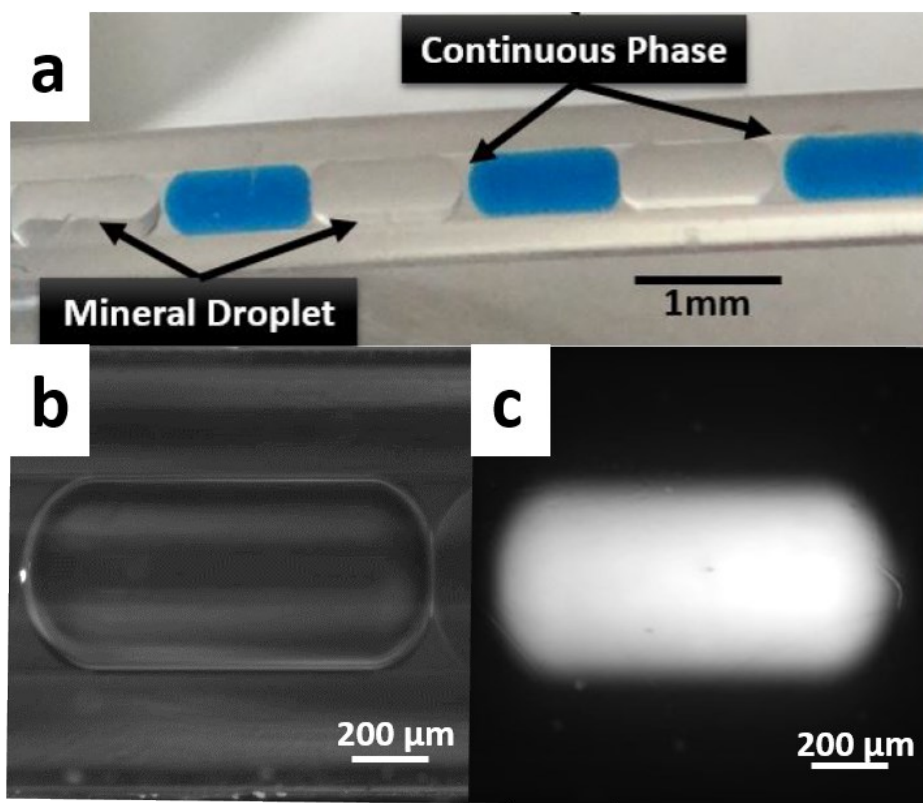


Fig. S16 The shape and size of droplets photographed by camera and microscopy. a) Droplet sequence generated by water-phase droplets (with blue dye), mineral oil spacer (transparent droplets), and continuous phase (HFE oil) with a flow rate ratio of 5:5:1 mL/h in the FEP tubing and photographed by a camera; b) Water-phase droplet (with Rhodamine dye) observed by microscopy under b) bright field and c) blue light.

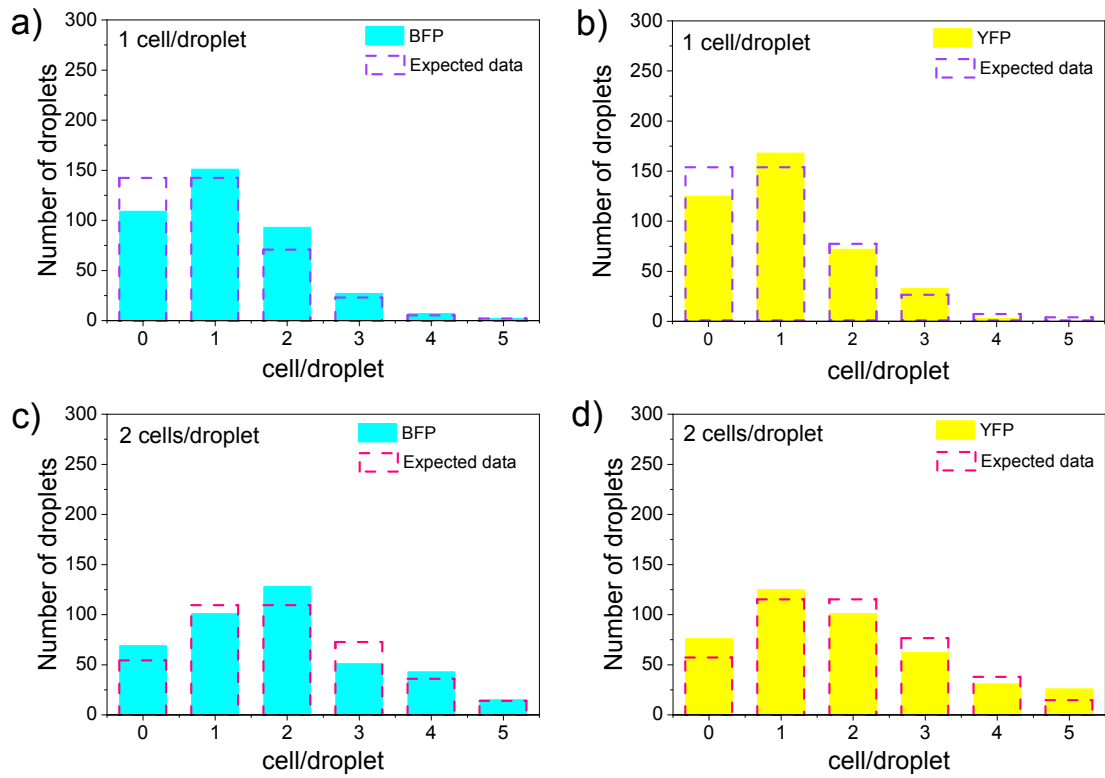


Fig. S17 Cell distribution of *E. coli BFP* and *E. coli YFP* with one or two cells in each droplet compared with the theoretical values of the Poisson distribution (dashed line). *E. coli BFP* with cell concentrations of a) one cell/droplet and c) two cells/droplet. *E. coli YFP* with cell concentrations of b) one cell/droplet and d) two cells/droplet.

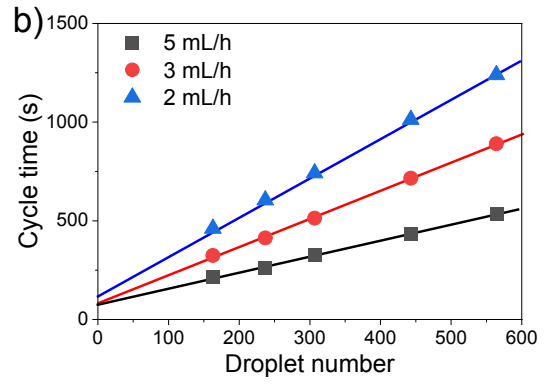
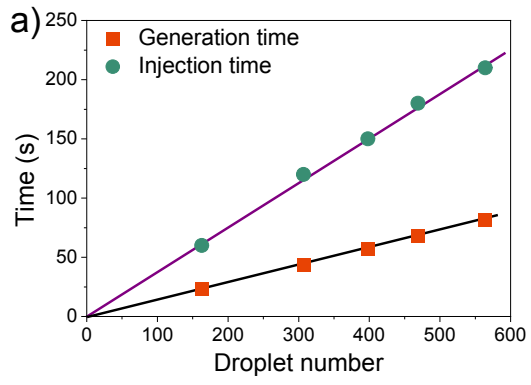


Fig. S18 Relationship between droplet number with a) generation and injection time, and b) cycle time.

Table S4. Comparison of light intensity and exposure time in different detection devices.

| Device | Millifluidic device | | Plate reader | | Flow cytometry | |
|-----------------|---------------------|----------|-------------------------------|-----|--------------------------|-------|
| | BFP | YFP | BFP | YFP | BFP | YFP |
| light intensity | 0.407 mW | 0.348 mW | not given (light power 5W) | | 50 mW | 50 mW |
| exposure time | 150 ms | | 25 ms | | depends on the flow rate | |

References

1. W. Z. Tim B. McAnaney, Camille F. E. Doe, Nina Bhanji, Stuart Wakelin, David S. Pearson, and X. S. Paul Abbyad, Steven G. Boxer, and Clive R. Bagshaw, *Biochemistry*, 2005, **44**, 5510-5524.
2. C. T. B. T. S. Karpova, L. He, X. Wu, A. Grammer, P. Lipsky, G. L. Hager and J. G. McNally, *Journal of Microscopy*, 2003, **209**, 56–70.
3. Y.-J. Yu, M. Amorim, C. Marques, C. Calhau and M. Pintado, *Journal of Functional Foods*, 2016, **21**, 507-516.
4. X. Zhang, X. Jiang, Q. Yang, X. Wang, Y. Zhang, J. Zhao, K. Qu and C. Zhao, *Anal Chem*, 2018, **90**, 6006-6011.